Comonomer Effect on the Mechanical and Morphological Behavior on the Calcite-Filled PP, CoPP, and TerPP

Hyun Kim,[1] Kwang Jae Kim,[1,2] Sang Min Kwon,[1] Patit P. Kundu,[1] Byung Cheon Jo,[3] Byung Hyung Lee,[3] Dae Soo Lee,[4] SoonJa Choe[1]

[1]*Department of Chemical Engineering, Inha University, Inchon 402-751, Korea*
[2]*R & D Center, Struktol, Stow, Ohio*
[3]*Taedok Institute of Technology, SK Corporation, Taejon 305-370, Korea*
[4]*Department of Chemical Engineering, Chonbuk National University, Cheounju 561-756, Korea*

Received 3 April 2001; accepted 15 February 2002

ABSTRACT: Comonomer effect on the mechanical and morphological behavior of the calcite (stearic acid coated calcium carbonate)-filled polypropylene (PP), poly(propylene-random-ethylene) copolymer (CoPP), and poly(propylene-*co*-ethylene-*co*-1-butene) terpolymer (TerPP) composites were investigated by using dumbbell bar and film specimens. The tensile properties of the calcite-filled PP, CoPP, and TerPP composites exhibited lower values than those of the pure polymers (calcite-unfilled polymers), whereas the complex viscosity of the calcite-filled polymers exhibited slightly higher values than that of the pure polymers. Mechanical properties studied by using various strain rates and draw ratios rationalized in terms of comonomer units and contents in various PP systems. Morphological behavior of the specimens stretched at various strain rates and draw ratios was investigated by using SEM microphotographs and the mechanism of the formation of air holes was proposed. The air hole initiated from crack propagation and followed by dewetting between the calcite surface and the polymer interface in the weakened region. The crack propagated along the transverse direction; then the air hole developed parallel to the machine direction with fibril structure of the resin in PP and CoPP systems. However, TerPP composite exhibited no cracks in the beginning of the elongation, but the air hole was initiated due to dewetting; then its enlargement was exhibited by broken fibril structure of the resin. In the final stage of stretching, the air hole was dominated by merging of the neighboring air holes. Thus, different comonomer units, which are the small content of ethylene and 1-butene in CoPP and TepPP, are responsible for these systems behaving in a different manner on the mechanical and morphological properties. J Appl Polym Sci 86: 2041–2053, 2002

Key words: composites; mechanical property; morphology; interface

INTRODUCTION

Mineral particles treated with interfacial agents, such as stearic acids and silanes, tend to wet or lubricate particle surfaces. Treated particles slide each other more than untreated ones and result reduced interparticle forces, viscosity, and agglomeration. An-isotropic particles such as fibers and flakes are easily oriented to the flow direction, yielding reduced particle–particle interactions at high shear. Some additives such as sulfur-added silane-coupling agents[1,2] and acrylamide[3] are examples.

Addition of mineral particles induces a significant increase in viscosity of composite materials. Compounding calcite into thermoplastic matrix has been studied by various researchers.[4–13] Calcite[6,7] is the most abundant mineral used as reinforcing particles because of its good dispersion in the thermoplastic matrix, but is also known as a moisture absorber.[8,10] Coating calcite with stearic acid was studied by various researchers[5,8,9,14–16] and is known to improve processibility during mixing with thermoplastics.[8,14] Few studies were employed on the stretching flow of these compounds[7–9] by using particles such as carbon black, calcite (calcium carbonate), and titanium dioxide; similar behavior was then reported at low strain rates. Calcite grafted with acrylamide improved the mechanical property of the high-density polyethylene (HDPE) compound.[7]

Wetting between polymers and filler particles was studied in terms of contact angle, surface and interfacial tension, and polarity, etc.[17–19] The best wetting characteristics of particles were reported when the contact angle becomes zero or less than zero. On the other hand, dewetting of particle-filled polymers is also important as much as wetting in the interfacial studies because it is widely applied and in demand for baby diapers and the sportswear industry because of its hydrophilic character[8,20,21] by use of polyethylene. Recently, calcite was used for baby diapers, but no

Correspondence to: S. Choe (sjchoe@inha.ac.kr).
Contract grant sponsor: Korea Science and Engineering Foundation (KOSEF); contract grant number: R01-2001-00432.

Journal of Applied Polymer Science, Vol. 86, 2041–2053 (2002)

TABLE I
Polyolefins Used in this Study

Olefin (grade name)	Density (g/cm^3)	MI (g/10 min)	HDT (°C)	Tensile strength (Kg/cm^2)	Code (comment)
Polypropylene (H 150)	—	7.5	154	370 (yield)	PP
*Co polypropylene (R930Y)	—	4.5	90	340	Co-PP PP:Ethylene (98:2 wt %)
*Ternary polypropylene (T131N)	—	5.0–5.5	60	230	Ter-PP PP:Ethylene: Butylene (93:2:5 wt %)

MI, melt index; HDT, heat distortion temperature.

reports of calcite-filled polypropylene (PP) composites were disclosed for the application of diapers or sportswear. Ventilation is one of the most important factors in manufacturing diapers. The most important factors on the ventilation of calcite-filled thermoplastics are known as crazing, dewetting, and the formation of air hole upon stretching.

Dewetting occurs when the surface of the particle is covered with a low surface tension material such as impurities or adsorbed water layers.[22] Because most engineering thermoplastics have higher surface tension, their use in combination with low surface tension material may induce a formation of dewetting or cracking.

Fillers are used for various purposes in thermoplastics. They are known not only to improve thermal, mechanical, electrical, and interfacial properties, but also to reduce production cost.[23,24] Calcium carbonate plays an important role as a reinforcing agent in the thermoplastic industry. It is well known that the addition of such a particulate influences a significant increase in the viscosity of thermoplastics. Experimental investigations of shear flow on rheological properties of calcium carbonate-filled polyolefin composites reported that the viscosity was augmented by several orders of magnitude at low shear rates, indicating the occurrence of yield values.[4–9,25]

We have investigated the mechanical and morphological properties of the deformed composites along various strain rates and draw ratios by using polyethylene systems.[24] In addition, the degree of mixing of the calcite particles in the HDPE, low-density polyethylene (LDPE), and linear low-density polyethylene (LLDPE) matrix was investigated.[26] There is no systematic research on the comparison between air hole and dewetting of particles separated from polymer matrices, in particular, with the use of the PP system. Thus, the objective of this study is to investigate the comonomer effect on the mechanical, rheological, and morphological properties upon stretching the calcite-filled PP, poly(propylene-random-ethylene) copolymer (CoPP), and poly(propylene-*co*-ethylene-*co*-1-butene) terpolymer (TerPP) systems. In addition, the mechanism of the air-hole formation and the possibility of controlling the air-hole size were also suggested by using morphological observation upon stretching of the film specimens.

EXPERIMENTAL

Materials

The three different polyolefins used in this study are PP, CoPP, and TerPP, supplied by SK Corp., Ulsan, Korea. CoPP contains 2 wt % ethylene comonomer in PP and TerPP contains 2 wt % of ethylene and 5 wt % of 1-butylene as comonomers in PP. The melting temperature of the above three polymers, PP, CoPP, and TerPP, is 166, 157, and 136°C, respectively, using DSC at 20°C of heating rate. Calcite used in this study is stearic acid coated SST-40 supplied by DOWA Co., Japan and their average particle size and the Brunauer, Emmett, and Teller (BET) surface area were 1.1 μm and 4.8 m^2/g, respectively. The information of the polyolefins and calcite used in this study are listed in Tables I and II.

Mixing and preparation of specimens

A Brabender PL 2000 Twin-Screw Extruder was used to compound calcite particles with PP, CoPP, and TerPP in a ratio of 50 : 50 wt %. Premixed calcite and polyolefins were fed into an extruder hopper and the compounded materials fed through an extruder die were pelletized. A temperature gradient was maintained in the barrel of the extruder that was 200°C at the feeding zone, 210°C at the compression zone,

TABLE II
Calcite Used in this Study

Calcite (grade name)	Density (g/cm^3)	Particle size (μm)	BET area (m^2/g)	Code (comment)
SST-40	2.9	1.1	4.8	Stearic acid treated calcite

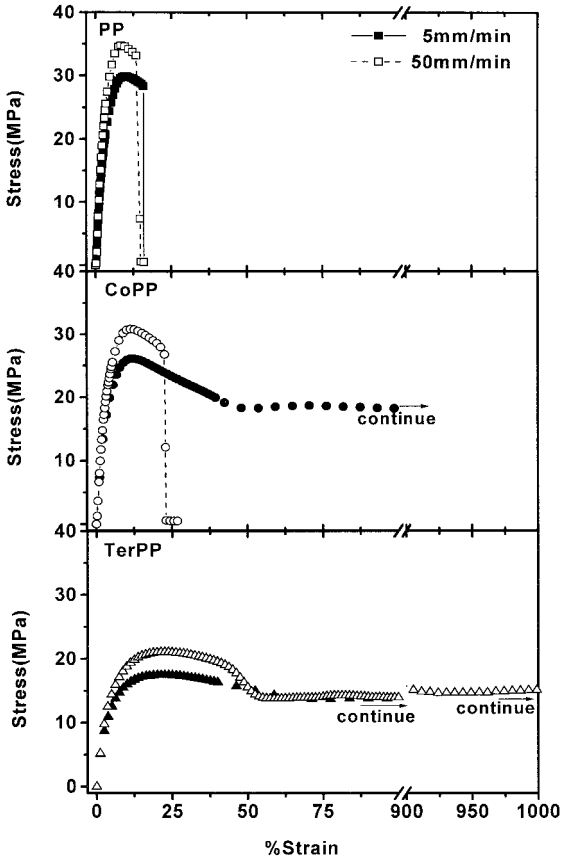

Figure 1 Stress–strain curves of the calcite-unfilled PP, CoPP, and TerPP dumbbell at 5 and 50 mm/min.

220°C at the metering zone, and 230°C at the die end for PP system. The operation temperature of the extruder was ambient from sample to sample (PP system at 230°C, CoPP and TerPP system at 220°C) and the screw rpm was kept at 70. The extruded materials were pelletized after passing through cold water at 20°C. To obtain consistent data, the specimens used were prepared by remixing the composite materials.

Dumbbell bar specimens having a dog-bone shape were prepared by melting the composite or the resin pellets on the mold plate by using a Carver laboratory hot press at 2×10^4 Pa and 200°C. Film specimens were prepared by using sheet extrusion with a slit die dimension 100×0.5 mm at 200°C. Extruded melt was pulled by using a take-up device and the film thickness was maintained at 0.4 mm. The 100-mm-width sheet was cut into 15×165 mm pieces. The dimensions of the dumbbell bar was $13 \times 3 \times 165$ mm because of the ASTM D638 (13×3 mm) and the dimensions of film was $15 \times 0.4 \times 165$ mm according to the ASTM D882-97 (15×0.4 mm).

Characterization

The tensile strength of film at yield and break and the elongation at break were measured by using an Instron 4301 at 20°C and 30% humidity. Both ends of the specimen were firmly tightened by upper and lower grip. The initial gap separation was 50 mm and the strain rate (i.e., gap-separation speed) was fixed at 5 and 50 mm/min for the dumbbell test. For the film test, two strain rates of 50 and 500 mm/min were used. To investigate quantitatively the crack propagation and the formation of the air hole, an initial gap distance of 10-mm-film per specimen was used, but only a 2-mm gap was investigated upon various draw ratios from 50 to 400% at 5 mm/min fixed strain rate.

At least 10 specimens were averaged to collect the tensile property. The morphology of the stretched film was studied by using SEM photographs and the interpretation was employed with the mechanical and SEM results.

A Hitachi S-4300 scanning electron microscope was used to obtain the image of calcite agglomerate in PP, CoPP, and TerPP matrix. The prepared composite specimen was fractured in liquid nitrogen and coated with silver by using a sputter coater. SEM microphotographs of each image were taken at ×1000 and ×2000 magnification. The side surface of the dumbbell bar or films was studied before and after stretching the specimen at ambient draw ratio and strain rate.

Complex melt viscosity of the compounds was measured by using a torsion rheometer Mk III from Poly-

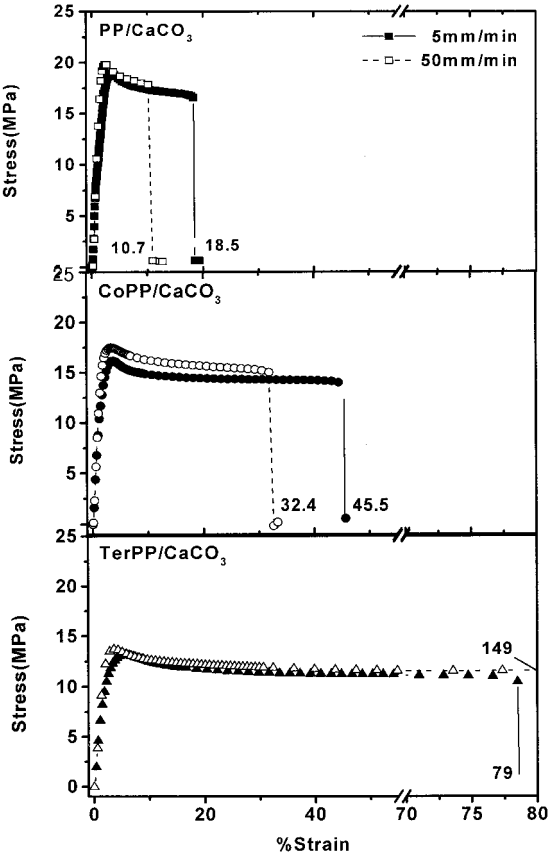

Figure 2 Stress–strain curves of the calcite-filled PP, CoPP, and TerPP dumbbell at 5 mm/min.

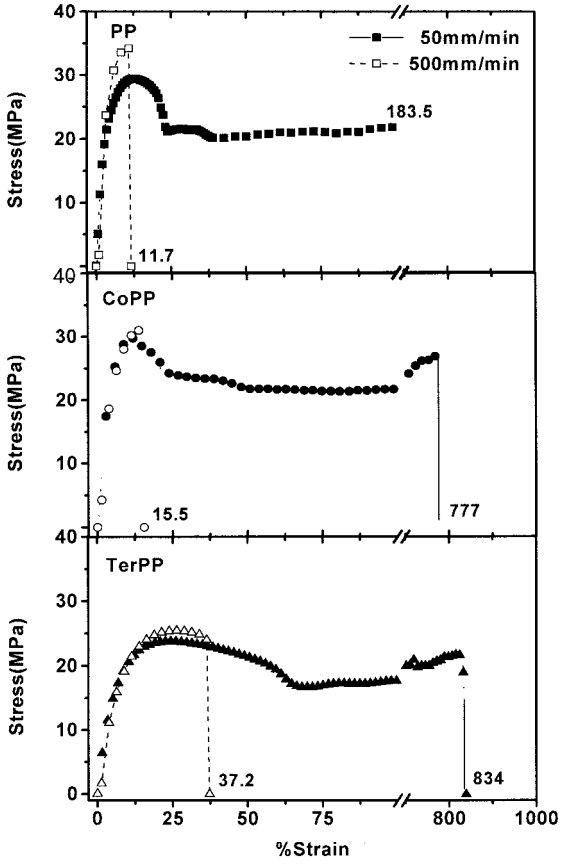

Figure 3 Stress–strain curves of the calcite-unfilled PP, CoPP, and TerPP film at 50 and 500 mm/min.

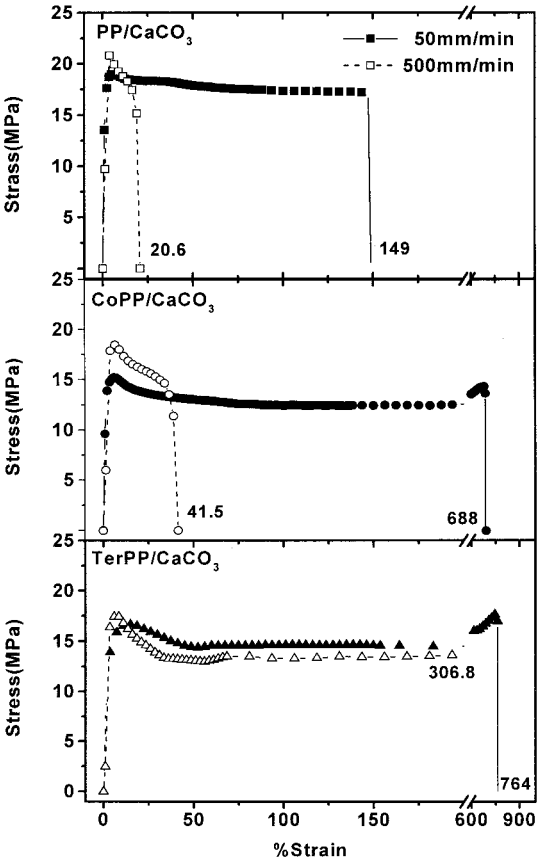

Figure 4 Stress–strain curves of the calcite-filled PP, CoPP, and TerPP film at 50 and 500 mm/min.

mer Laboratories. After strain sweep, the complex viscosity of the compounds was measured in a parallel plate (D = 38 mm) over a frequency range of 0.03 to 200 s^{-1}. The strain amplitude was maintained constant at 4% for all measurements.

The shear stress for sinusoidal oscillatory flow experiments had the form

$$\sigma_{12}(t) = G'(\omega)\gamma \sin \omega t + G''(\omega)\gamma \cos \omega t = G^*\gamma \sin(\omega t + \delta) \quad (1)$$

where γ is the shear strain, G' is the shear storage modulus, G^* is the shear complex modulus, ω is the frequency, and δ is the loss angle. The torque (M) was related to the shear stress $\sigma_{12}(R)$ at the outer radius by

$$G'(\omega) = G^* \cos\delta = \frac{2MH}{\pi R^4 \theta}\cos\delta \quad (2)$$

$$G'(\omega) = G^* \sin\delta = \omega\eta' = \frac{2MH}{\pi R^4 \theta}\sin\delta \quad (3)$$

$$\eta^* = \sqrt{(\eta')^2 + (\eta'')^2} = \sqrt{\left(\frac{G''}{\omega}\right)^2 + (\eta'')^2} = \frac{G^*}{\omega} \quad (4)$$

The strain γ at the outer radius was $R\Delta\theta/h$, where R is the plate radius, H is the gap height, and θ is the shear angle.

RESULTS AND DISCUSSION

Mechanical test

To compare the tensile property between the calcite-unfilled and -filled PP with its derivative compounds, stress–strain behavior of the unfilled systems was also observed. Figure 1 represents the calcite-unfilled (pure

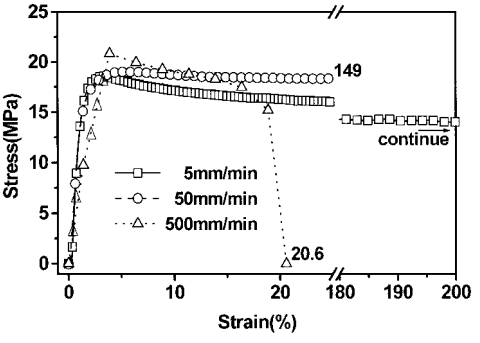

Figure 5 Tensile stress–strain curves of the calcite-filled PP films stretched at 5, 50, and 500 mm/min.

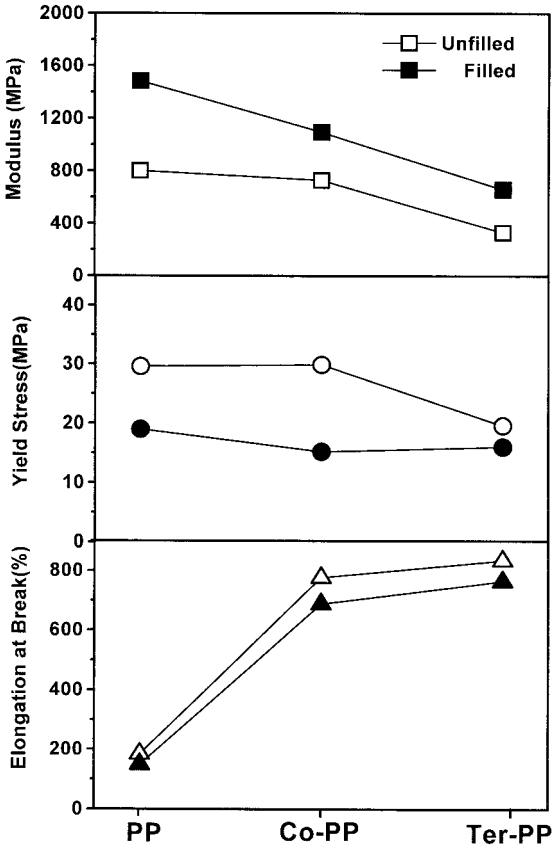

Figure 6 Modulus, yield stress, and elongation at break of calcite-unfilled and -filled PP, CoPP, and TerPP composites film at 50 mm/min (open symbol; unfilled, solid symbol; filled).

polymers) PP, CoPP, and TerPP dumbbell bar stretched at different strain rates at 5 and 50 mm/min with error bars, indicating experimental deviations. As the strain rate augmented from 5 to 50 mm/min, the yield stress increased from 30 to 35 MPa for PP, from 27 to 32 MPa for CoPP, and from 17.5 to 22 MPa for TerPP. As usual, this indicates that the higher the strain rate, the higher the yield stress is observed. On the other hand, for the elongation at break, no distinctive difference was observed in PP between two different strain rates, but decreased with the strain rate in CoPP, whereas no difference was observed because of the experimental condition under the given machine limit for TerPP. In addition, the stress–strain curves of the calcite-filled PP, CoPP, and TerPP composites for dumbbell specimen at strain rates of 5 and 50 mm/min are presented in Figure 2. For the tensile property at 5 mm/min, the observed yield stress of PP, CoPP, and TerPP dumbbell bar was 19, 17, and 13.5 MPa, the tensile stress at break was 17, 14.5, and 12 MPa, and the elongation at break was 18.5, 45.5, and 149%, respectively. The elongation at break increased, but the yield stress and the tensile strength at break decreased with the comonomer content in PP matrix. Although we have not presented the results obtained from the initial mixing, tensile property prepared by remixing exhibited relatively consistent data than by the initial mixing, which implies that remixing improves homogeneity. For the tensile property at 50 mm/min, the yield stress for PP, CoPP, and TerPP dumbbell exhibited 20, 18, and 14 MPa, respectively. The tensile strength at break was 18, 15, and 12.5 MPa, and the elongation at break was 11, 32, and 79%, respectively. As the same trend as seen in the Figure 1, the yield stress and the stress at break decreased with the strain rate, but this trend reversed in the elongation at break. Because we were more interested in film property for its application, the investigation was continued using film specimens.

The stress–strain curves of calcite-unfilled PP, CoPP, and TerPP film measured at 50 and 500 mm/min are shown in Figure 3. The observed yield stress of PP, CoPP, and TerPP at 50 mm/min was 30, 30, and 24 MPa; the tensile strength at break was 23, 27, and 24 MPa, and the elongation at break was 184, 777, and 834%, respectively. In addition, the yield stress of PP, CoPP, and TerPP films at 500 mm/min was 34.5, 32, and 26.5 MPa, the tensile strength at break was 33, 30, and 24 MPa, and the elongation at break was 12, 16, and 37%, respectively. The yield stress and stress at break at high shear rate were higher than those at low shear rate, but the elongation at break exhibited reversion behavior to the stress.

Figure 4 presents the stress–strain curves of the calcite-filled PP, CoPP, and TerPP film measured at 50 and 500 mm/min. The yield stress of PP, CoPP, and TerPP at 50 mm/min was 19, 16, and 17 MPa; the tensile strength at break was 16, 15, and 18 MPa, and the elongation at break was149, 688, and 764%, respectively. In addition, the yield stress of PP, CoPP, and TerPP at 500 mm/min was 21, 18.5, and 17.5 MPa; the tensile strength at break was 17.5, 15, and 13 MPa, and the elongation at break was 21, 41.5, and 307%, respectively. The trend for the yield stress, the stress at break, and the elongation at break at high shear rate was the same as the calcite-unfilled systems seen in Figure 3.

Figure 5 presents the stress–strain curves of the calcite-filled PP film at various strain rates at 500, 50, and 5 mm/min. The yield stress was 21, 19, and 18 MPa; the tensile strength at break was 16.5, 16, and 14 MPa, and the elongation at break was 21, 149, and $>$ 200%, respectively. By comparison, PP data between three different strain rates, the higher the strain rate, the higher the yield stress but the lower the elongation were observed.

The modulus, the yield stress, and the elongation at break of the calcite-unfilled and -filled films of PP, CoPP, and TerPP systems at 50 mm/min are compared in Figure 6. The modulus of calcite-filled PP and its derivatives were higher than the calcite-unfilled

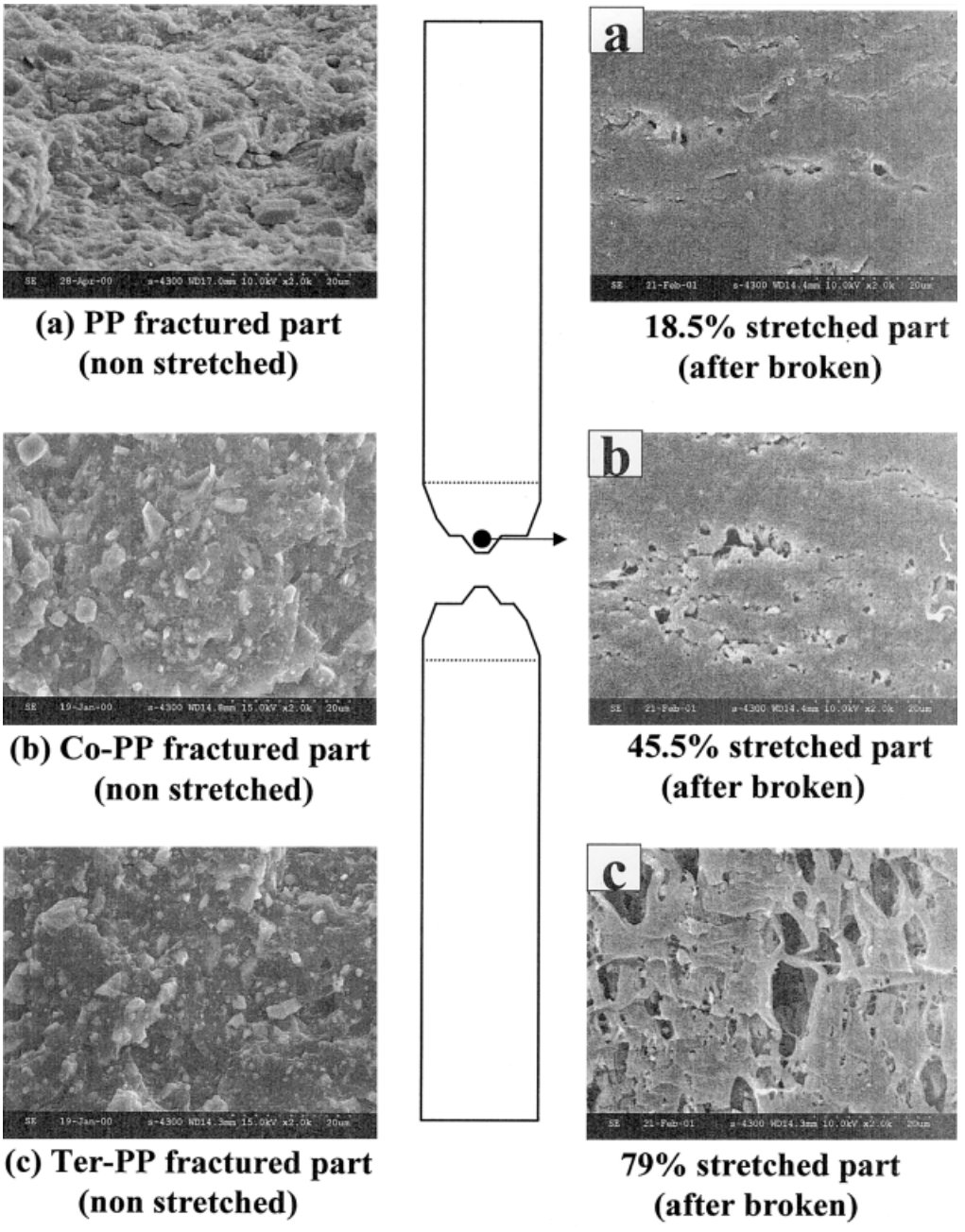

Figure 7 SEM photographs between the fractured and stretched part at 5 mm/min of the calcite-filled PP (a), CoPP (b), and TerPP (c) systems with dumbbell shape.

composites, which means that the calcite-filled systems are more rigid than the unfilled ones. However, the yield stress of the filled composites was lower than the pure (unfilled) polymers, indicating that there is no reinforcing effect in these systems. We assume that the interfacial force between the PP matrix and the stearic acid coated calcium carbonate particles is weak. On the other hand, the elongation at break for the pure PP, CoPP, and TerPP film was 184, 777, and 834%, but that for the calcite composite was 149, 688, and 764%. The yield stress, tensile strength at break, and elongation of the calcite-filled PP, CoPP, and TerPP composite were slightly reduced. This implies that the comonomer ethylene in CoPP and ethylene and 1-butene in TerPP are responsible for giving different mechanical properties, which gives reduced modulus and yield stress, but increased elongation at break.

Morphology by SEM observation

The fractured surface after broken in the atmospheric liquid nitrogen chamber and the broken surface after ambient stretching using the remixed calcite filled PP, CoPP, and TerPP dumbbell bar are exhibited in the

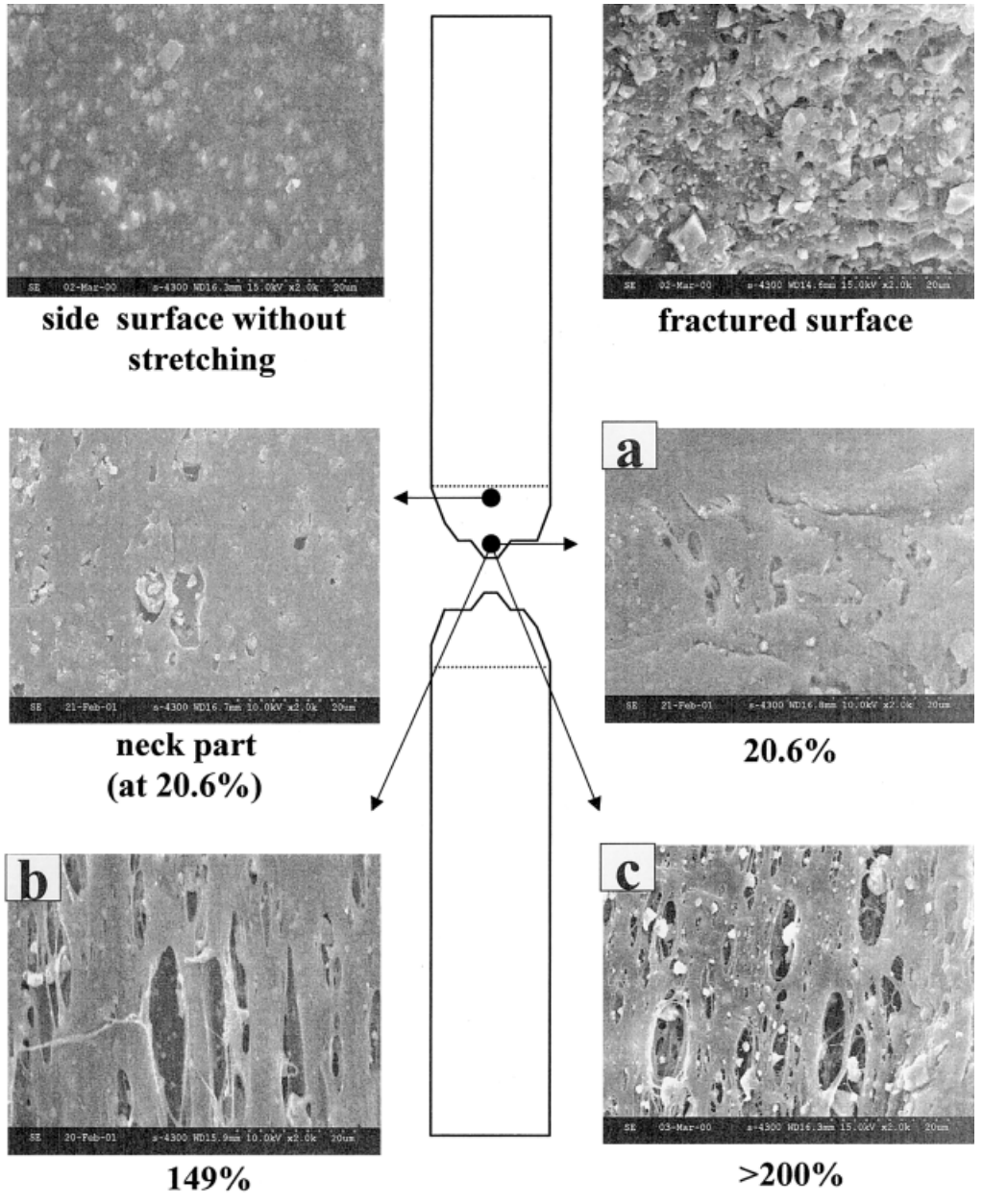

Figure 8 SEM photographs of the PP/$CaCO_3$ film at broken side surface stretched at (a) 500 mm/min, (b) 50 mm/min, (c) 5 mm/min.

left-hand and right side of the Figure 7(a–c) and 7(a′–c′), respectively. This is the part drawn in the specimen of Figure 7. No significant difference was observed in the calcite agglomerate size or in the degree of mixing between three compounds. The right-hand side of Figure 7(a′–c′) presents the broken surface of the dumbbell bar, where the PP composite was broken at 18.5% elongation, CoPP was broken at 45.5%, and TerPP was broken at 45% elongation, respectively. As seen in Figure 7(a′,b′), cracking was observed along the transverse direction of the specimen when broken. In particular, a formation of the air hole was observed in the interface between the calcite particles and the PP, CoPP, and TerPP resin. This phenomenon was also observed by using film specimens and will be discussed in detail later.

Because the elongation of the calcite-filled PP composite is very small at 500 mm/min, the strain rate-dependent phase morphology after break by using PP system was studied. The specimens were stretched at 500, 50, and 5 mm/min and compared the broken surface with 21, 451, and >200% of elongation as in Figure 8(a–c), respectively. Crack propagated along the transverse direction when the PP specimen stretched at 500 mm/min and this behavior was predominant when the elongation was small. However, when the PP composite stretched with slow strain rate as seen in Figure 8(b) or 8(c), dewetting and a simul-

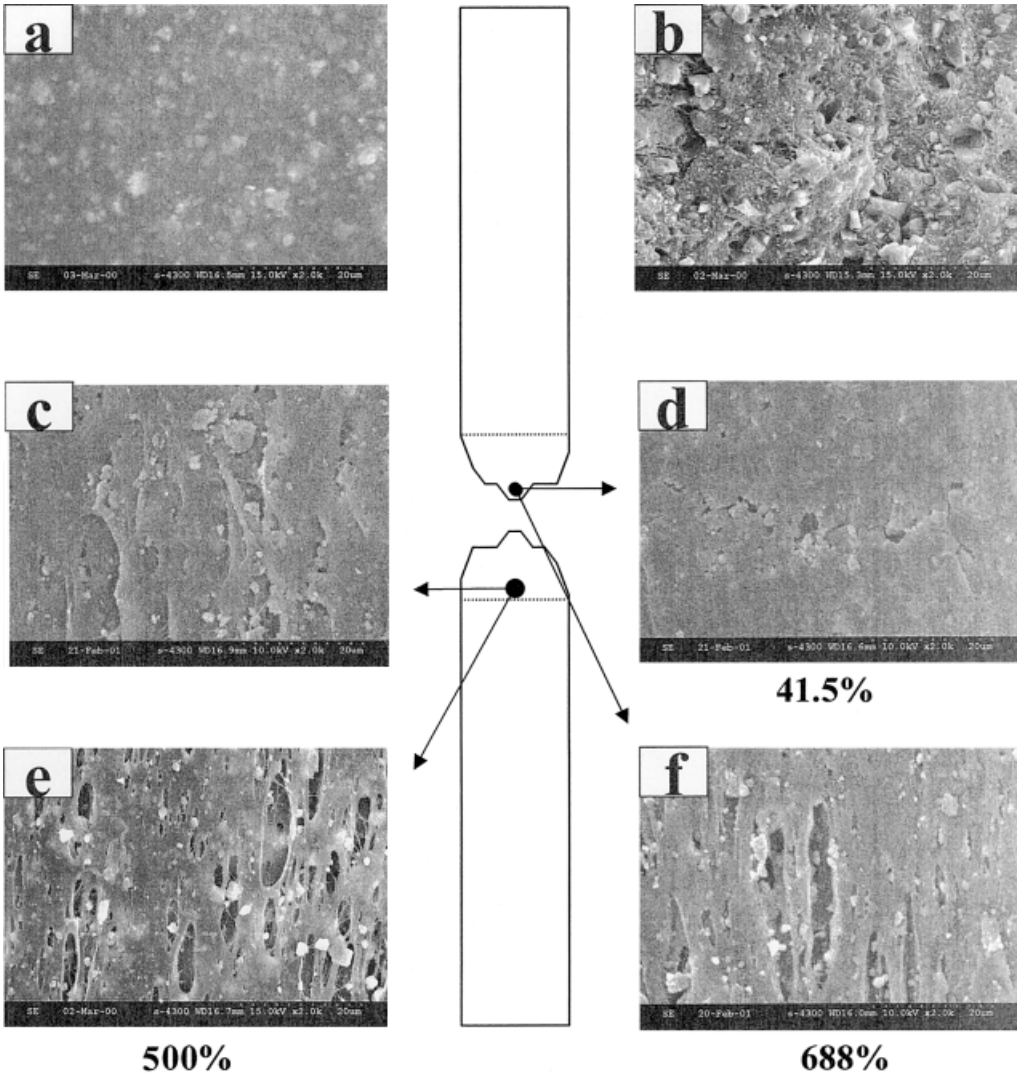

Figure 9 SEM photographs of the CoPP/$CaCO_3$ film (a) side surface without drawing, (b) fractured surface, (c) neck part (500 mm/min), and side surface at (d) 42% (500 mm/min), (e) 500% (50 mm/min), (f) 688% (5 mm/min).

taneous enlargement of the air hole were observed with a fibril structure. This result tells us that the phase morphology of the broken surface is quite dependent on the strain rate. Thus, it is suggested that the air hole in PP composites can be controlled by varying strain rates and stretching conditions such as temperature augmentation.

Calcite-filled CoPP and TerPP composites were stretched with an initial gap distance of 10 mm and compared the phase morphology between the neck part and the elongated middle part of the specimen. The observed phase morphology of the calcite-filled CoPP film in the side and the fractured surface without stretching is seen in Figure 9(a,b). Figure 9(c,d) represents the neck and broken surface of the calcite-filled CoPP composite stretched at 500 mm/min, respectively. Because the strain rate was very high (500 mm/min), the specimen was broken at 42% elongation and the phase morphology between the neck and the broken part was quite different. No crack was observed in Figure 9(c), but crack propagation was observed toward the transverse direction (TD) in Figure 9(d), instead a formation of the air hole dominated because of dewetting between the calcite particles and the resin matrix. When the film specimen stretched at a relatively low strain rate of 50 mm/min, small-sized air holes formed from dewetting between the interface of the calcite and the resin matrix in Figure 9(e). Then air holes enlarged not only by breaking the fibril structure, but also by merging air holes as seen in Figure 9(f).

In addition, for the TerPP system, the morphology of the side surface of the unstretched specimen and the fractured surface is almost the same as the CoPP system, as in Figure 10(a,b), respectively. When the specimen stretched at high draw rate (500 mm/min), as seen in Figure 10(c), some of the air holes were observed without the formation of a crack in the neck

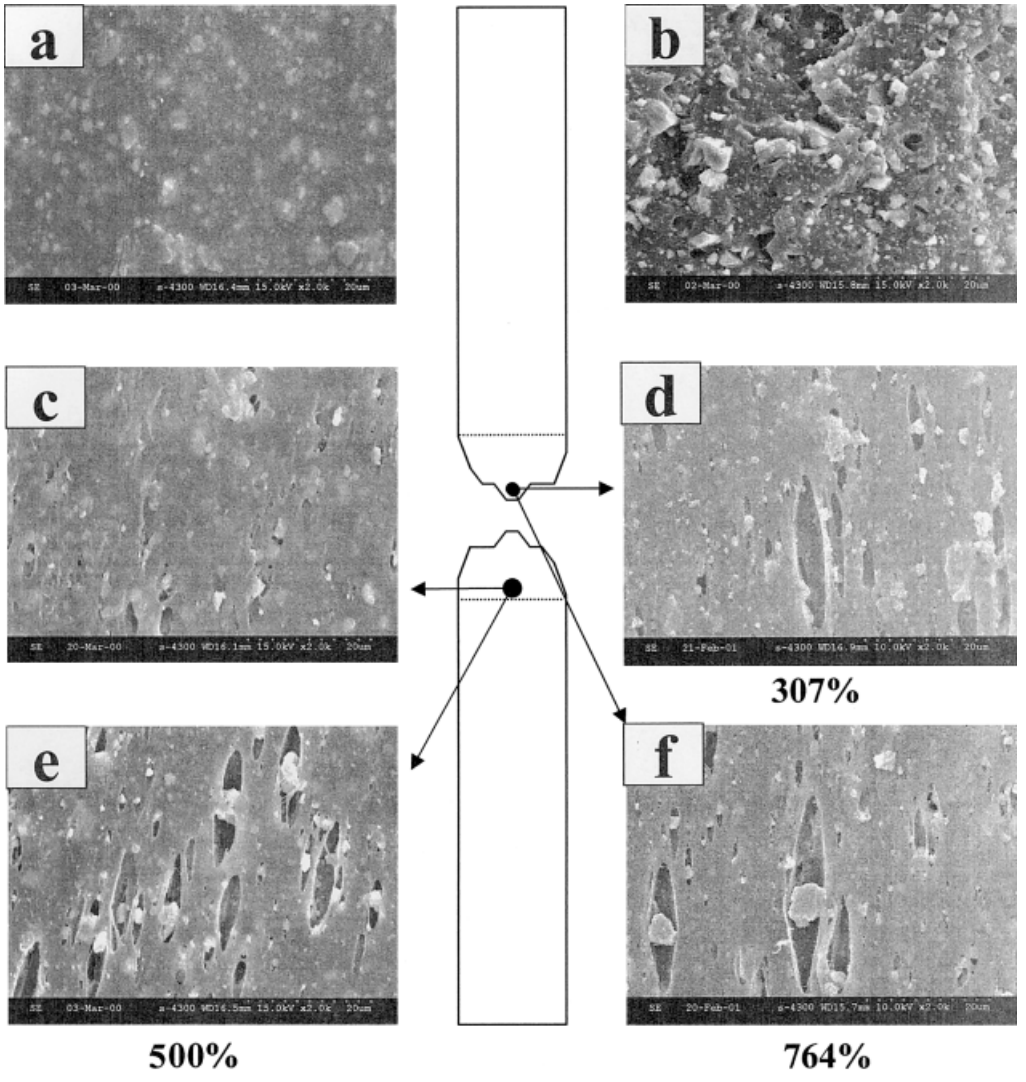

Figure 10 SEM photographs of the TerPP/$CaCO_3$ film (a) side surface without drawing, (b) fractured surface, (c) elongated neck part (500 mm/min), and side surface at (d) 307% (500 mm/min), (e) 500% (50 mm/min), (f) 764% (5 mm/min).

part. In addition, when the TerPP composite was stretched at 500 mm/min and broken at 307% elongation, a long ellipsoidal shape of the air hole was exhibited along the machine direction (MD), as seen in Figure 10(d). On the other hand, when the specimen stretched lower draw ratios at 50 mm/min, most of the air holes seemed to be initiated from dewetting behavior with 500% elongation [Fig. 10(e)]. As the elongation increased up to 764% as in Figure 10(f), the broken fibril structure of the matrix, followed by a merging of small air holes, was responsible to form larger air holes. The comonomers contained in CoPP and TerPP are ethylene and ethylene with 1-butene, respectively; thus, 1-butene is expected to affect in flexibility more than ethylene when it is attached in the side chain. Therefore, the more the flexible comonomer content, the more elongation and the less fibril structure were observed due to an addition of flexible ethylene or 1-butene units into PP structure. The crack propagation in PP and CoPP systems may be influenced by propylene-rich PP and CoPP systems.

Films were quantitatively stretched at a constant strain rate of 5 mm/min with various draw ratios in order to study the formation of a crack and the development of the air hole from dewetting. SEM photographs of the calcite-filled PP, CoPP, and TerPP composites with different draw ratios are shown in Figures 11, 12, and 13, respectively. When the initial stretching was applied between 50 and 75% in PP system, as seen in Figure 11, the crack along the transverse direction and the air holes along the machine direction were simultaneously formed. This may arise from dewetting between PP resin and the calcite particles due to the weak interfacial force between these. Then, from 100 to 300% of draw ratio, the size and the number of the air holes gradually increased. At this draw ratio, the tearing of the fibril structure and merg-

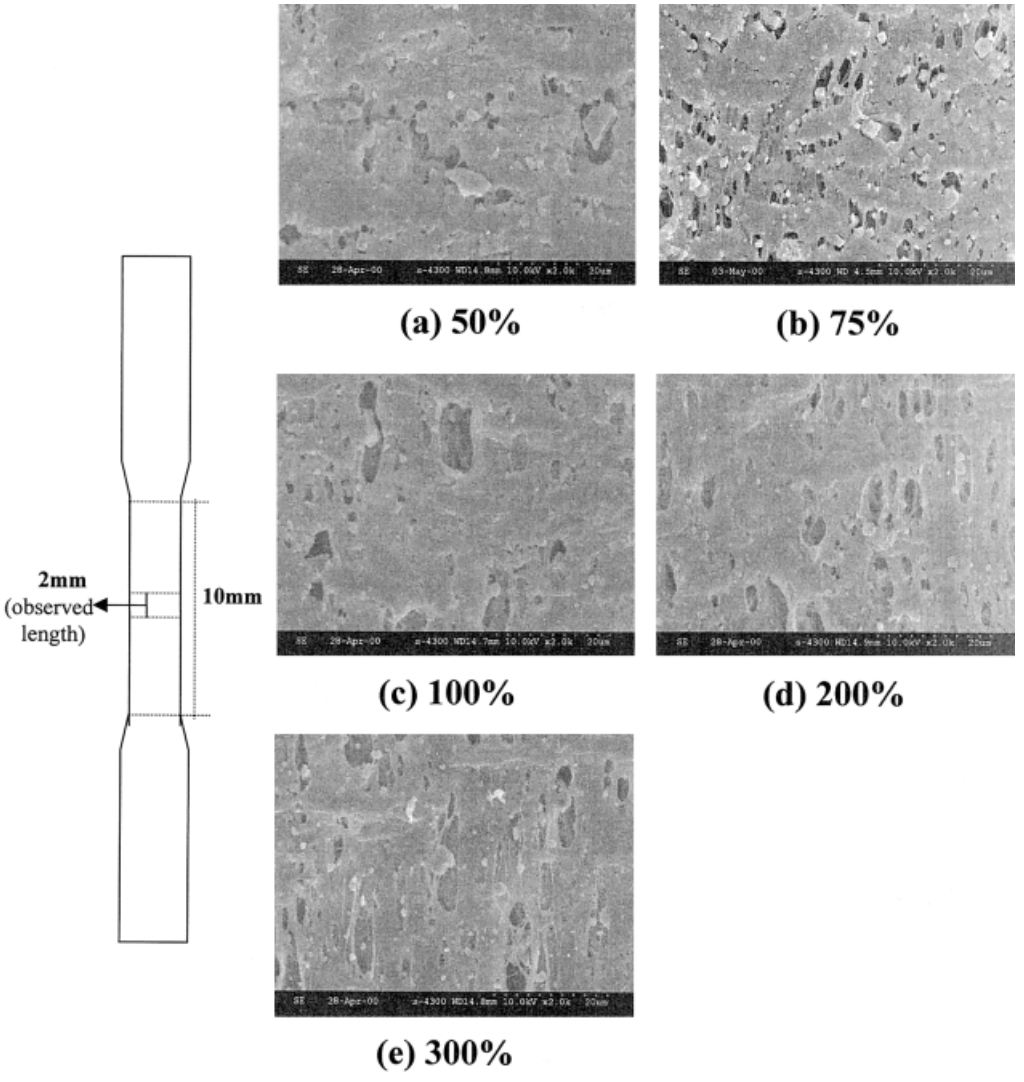

Figure 11 SEM photographs of the PP composite film side surface stretched at 5 mm/min. The initial gap distance is 10 mm, but the observed length in 2 mm, and the numbers represent the strain rate.

ing effect of each air hole dominated, and as a result, the ellipsoidal shape of air holes was obtained. For the CoPP composite, as shown in Figure 12, no crack was observed between 50 and 400% of the draw ratio, unlike the PP system, which may arise from the comonomer ethylene content. As the draw ratio increased, the size and the number of the air holes gradually increased and the formation of dewetting and fibril structure were also observed. In addition, with TerPP composite in Figure 13, almost the same behavior as CoPP was observed. At low draw ratios between 50 and 200%, the air hole was mainly formed by dewetting; however, at high draw ratios over 200%, the air hole enlarged by not only breaking the fibrous structure of the resin, but also by the merging effect between air holes. Fibril structure is dominant in PP, CoPP, and TerPP composites at high draw ratios and this affects the formation of enlarged air holes. Fibril structure was also observed in the calcite-filled HDPE composites studied earlier in this laboratory.[15]

Rheological measurements

The complex melt viscosity (η^*) of the calcite-unfilled and -filled PP, CoPP, and TerPP composites was summarized in Figure 14 as a function of frequency (ω) at an amplitude of 4% strain. For the calcite-unfilled system, which is pure polymer, CoPP exhibited the highest viscosity for all over the frequency range, TerPP follows next and then PP compounds. For the calcite-filled system, the viscosity was slightly higher than that of unfilled one but is not distinctive. As observed in the mechanical properties, the calcite-filled composite showed rather decreased property, implying that no reinforcing effect of the calcite in PP

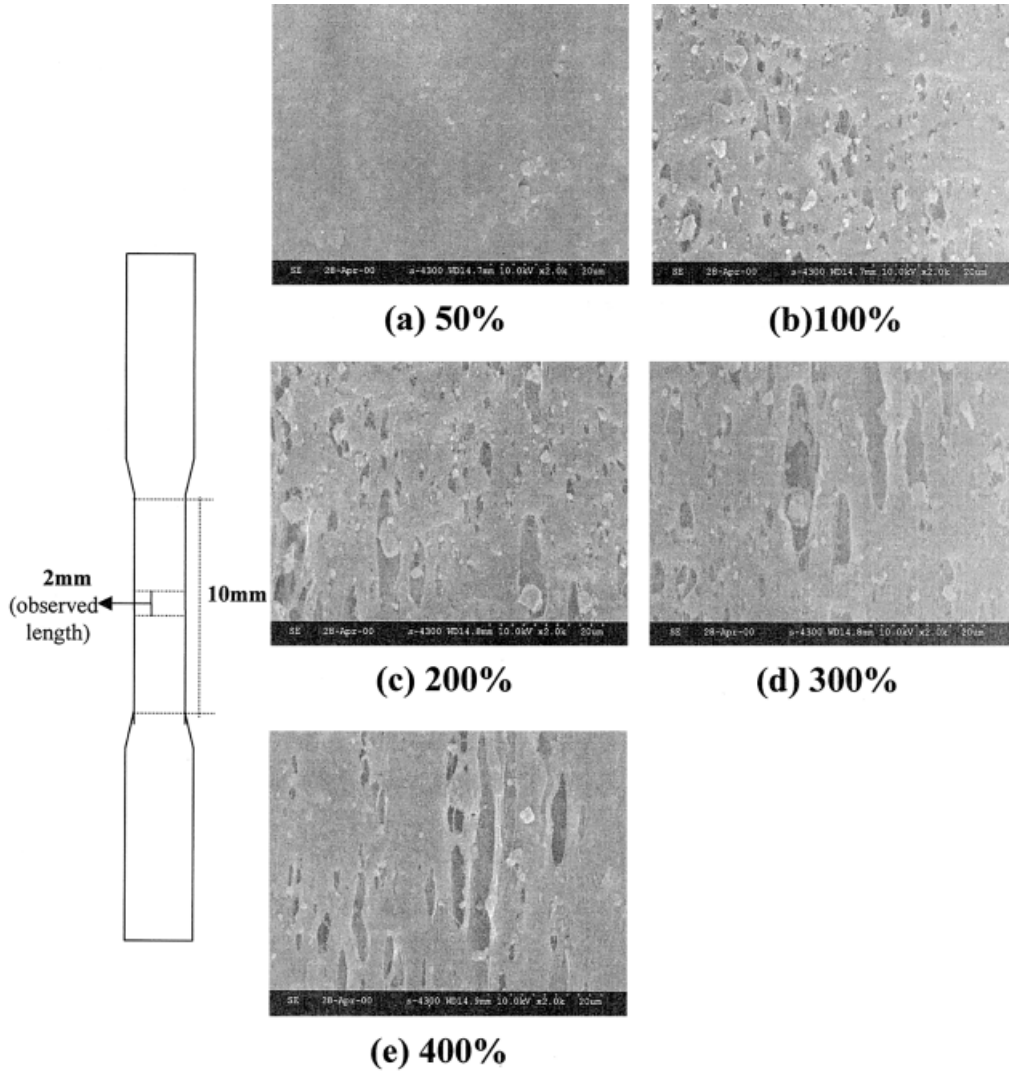

Figure 12 SEM photographs of the CoPP composite film side surface stretched at 5 mm/min. The numbers and the observed length represent the same manner as in Figure 11.

and its derivative compounds appears. In addition, no yielding value was observed in our investigated systems.

CONCLUSION

The comonomer effect on the mechanical and phase morphological behavior of the calcite (coated with stearic acid)-filled PP, CoPP, and TerPP composites was investigated by using a dumbbell bar and film specimens. The tensile properties of the calcite-filled PP, CoPP, and TerPP composites exhibited lower values than those of the pure polymers (calcite-unfilled polymers), whereas the complex melt viscosity of the calcite-filled polymers exhibited slightly higher than that of the pure polymers. This indicates that there is no reinforcement effect on the calcite particles with PP compounds. Mechanical properties were studied by using various strain rates and draw ratios, and the experimental results rationalized in terms of comonomer units and contents in PP and its derivative systems. Morphological behavior of the specimens stretched at various strain rates and drawing ratios was studied and the mechanism of the formation of air holes was proposed. The air hole initiated from crack propagation and was followed by dewetting between the calcite surface and the polymer interface in the weakened region. The crack propagated along the TD; then, the air hole developed parallel to the MD with fibril structure of the resin in PP, CoPP, and TerPP systems. However, TerPP composite exhibited no cracks in the beginning of the elongation, but the formation of air holes because of dewetting and its enlargement by broken fibril structure of the resin and the merging effect of the air holes were dominant in the later elongation. Thus, different comonomer units, which are the small content of ethylene and 1-butene in CoPP and TepPP, are responsible for bringing a

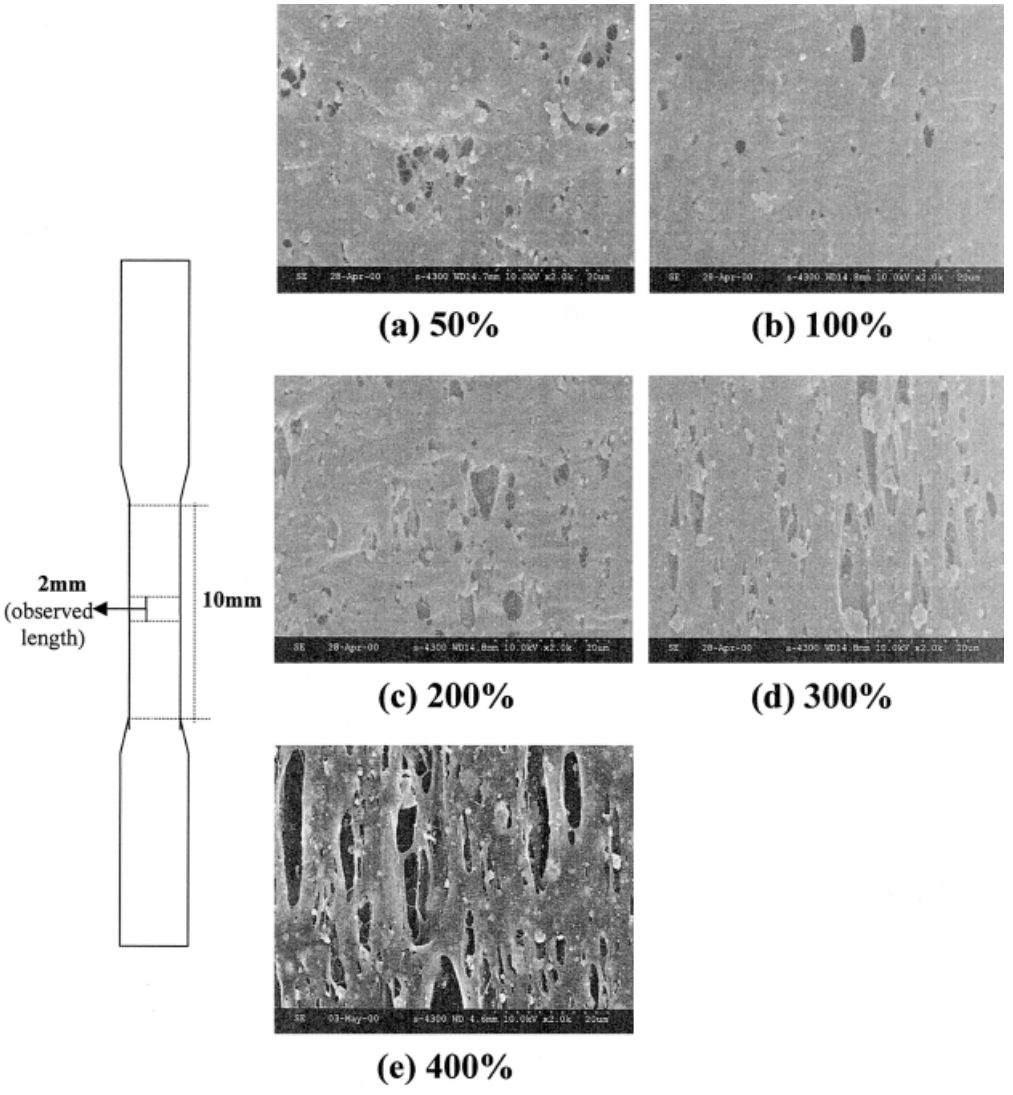

Figure 13 SEM photographs of the TerPP/composite film side surface stretched at 5 mm/min. The numbers and the observed length represent the same manner as in Figure 11.

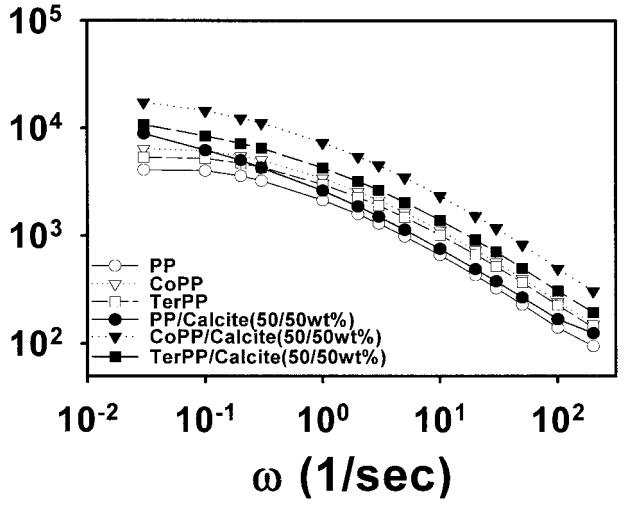

Figure 14 Complex melt viscosity as a function of frequency for pure PP, CoPP, and TerPP, and the calcite-filled PP, CoPP, and TerPP systems at 240°C.

different behavior of the mechanical and morphological properties.

This work was supported KOSEK, grant number: R01-2001-00432 and was partially supported by SK Corporation. In particular, Dr. Patit P. Kundu thanks KOSEF and Inha University for a chance to work as a postdoctoral fellow.

References

1. Kataoka, T.; Kitano, T.; Sasahara, M.; Nishijima, K. Rheol Acta 1978, 17, 149.
2. Kataoka, T.; Kitano, T.; Oyanagi, Y.; Sasahara, M. Rheol Acta 1979, 18, 635.
3. Tanaka, H.; White, J. L. Polym Eng Sci 1980, 20, 949.
4. Wang, Y.; Lu, J.; Wang, G. J Appl Polym Sci 1997, 64, 1275.
5. Suetsugu, Y.; White, J. L. J Appl Polym Sci 1983, 28, 1481.
6. Kim, K. J.; White, J. L. J Non-Newt Fluid Mech 1996, 66, 257.
7. Kim, K. J.; White, J. L. Polym Eng Sci 1999, 39, 2189.
8. Kim, K. J. Ph.D. Dissertation. Rheology, processing, and characterization of isotropic, anisotropic, and mixed particle filled polymer system; Univ. of Akron, 1998.

9. Kim, K. J.; White, J. L.; Choe, S.; Dehennau, C. to appear.
10. Harrington, E. A. Am J Soc 1927, 13, 467.
11. Chacko, V. P.; Karasz, F. E.; Farris, R. J. Polym Eng Sci 1982, 22, 968.
12. Chacko, V. P.; Farris, R. J.; Karasz, F. E. J Appl Polym Sci 1983, 28, 2701.
13. Banhegyi, G.; Karasz, F. E. J Polym Sci: Polym Phys Ed 1986, 24, 209.
14. Araki, T.; White, J. L. Nihon Reoroji Gakkaishi to appear.
15. McGenity, P. M.; Hooper, J. J.; Paynter, C. D.; Riley, A. M.; Nutbeem, C.; Elton, N. J.; Adams, J. M. Polymer 1992, 33, 5215.
16. White, J. L.; Czarnecki, L.; Tanaka, H. Rubber Chem Technol 1980, 53, 823.
17. Sheldon, R. P. Composite Polymeric Materials; Applied Science Publishers: London, 1982.
18. Wu, S. Polymer Interface and Adhesion; Dekker: New York, 1982.
19. Li, L. L.; White, J. L. Rubber Chem Technol 1996, 69, 628.
20. Banhegyi, G.; Karasz, F. E. Polym Eng Sci 1990, 30, 374.
21. Harrington, E. A. Am J Soc 1927, 13, 467.
22. Yosomiya, R.; Morimoto, K.; Nakajima, A.; Ikada, Y.; Toshio, S. Adhesion and Bonding in Composites; Dekker: New York, 1989.
23. White, J. L. Rubber Processing: Technology, Materials, and Principles; Hanser Publishers: Cincinnati, OH, 1995.
24. Kwon, S.; Kim, K. J.; Kim, H.; Kim, T.; Lee, Y. K.; Lee, B. H.; Choe, S. Polymer, accepted.
25. McNeish, A. A.; Byers, J. T. Low Rolling Resistance Tread Compounds—Some Compounding Solutions; Degussa Corp., ACS Rubber Division Meeting, Anaheim, CA, May 1997.
26. Kim, K. J.; Kwon, S.; Kim, H.; Jo, B. C.; Lee, Y. K.; Lee, K. J.; Lee, B. H.; Choe, S. J Appl Polym Sci, accepted.